Engel (28)
Study No. H81 3345

CHARACTERISTICS OF THE WSC BASKET TYPE BED LOAD SAMPLER

By

Peter Engel

Environmental Hydraulics Section
Hydraulics Division
National Water Research Institute
Canada Centre for Inland Waters

October 1982

TABLE OF CONTENTS

SUMMARY

Using dimensional analysis, the sampler catch and sampling efficiency of the WSC basket type bed load sampler were expressed in terms of flow condition, sediment properties and sampler geometry. Existing data and new data obtained in a large sediment flume, using scale models of the sampler, were used to examine the effects of the pertinent independent variables. The sampler catch was found to increase with the sampling time $t_* U_* / L_b$ (t_* = sampling time, U_* = shear velocity, L_b = length of the sampler), with the mobility number $\rho U_*^2 / \gamma_s D_{50}$ (ρ = density of water, γ_s = submerged unit weight of sediment), the relative grain size D_{50}/L_a and the grain size distribution factor ψ ($\psi = D_{84}/D_{16}$). The sampling efficiency was found to depend on $t_* U_* / L_b$ and D_{50}/L_a. When $D_{50}/L_a > 0.048$, the sampling efficiency was found to depend on $t_* U_* / L_b$ only. For practical application, a sampling efficiency of 30% may be used when $30 \leq t_* U_* / L_b \leq 90$.

RÉSUMÉ

On a utilisé l'analyse dimensionnelle pour exprimer le volume de prise et le rendement de l'échantillonneur de charge de fond en forme de panier de la D.R.H.C. en fonction des conditions d'écoulement, des propriétés des sédiments et de la géométrie de l'échantillonneur. Des données existantes et de nouvelles données recueillies dans un grand bassin sédimentologique à l'aide de maquettes et l'échantillonneur ont permis d'étudier les effets des variables indépendantes pertinentes $t_* U_*/L_b$ (t_* = temps d'échantillonneur), du facteur de mobilité $\rho U_* U^2/T_s D_{50}$ (ρ = masse volumique de l'eau, T_s = masse volumique immergée des sédiments), du diamètre relatif des grains D_{50}/L_a et du facteur de répartition granulométrique ψ ($\psi = D_{84}/D_{16}$). Le rendement d'échantillonnage est fonction de $t_* U_*/L_b$ et de D_{50}/L_a. Lorsque $D_{50}/L_a > 0{,}0048$, le rendement est fonction de $t_* U_*/L_b$ seulement. En pratique, on peut estimer à 30% le rendement lorsque $30 \leq t_* U_*/L_b \leq 90$.

MANAGEMENT PERSPECTIVE

This study was undertaken to examine the concerns of the Water Survey of Canada in the use of basket type samplers to estimate sediment transport in rivers as bed load.

The results show that the ratio of the measured rate to the actual rate remains constant over a range in values of a controlling dimensionless variable $t_* V_* / L_b$. When this variable is greater than 30, then the efficiency is 30%.

Present practice in sampling is to adopt 30% as the efficiency and this practice is confirmed. However, operating procedures should ensure that sampling times are selected to make $t_* V_* / L_b$ greater than 30 and not more than 90.

In that expression:

t_* is the sampling time in seconds

L_b is the length of the sampler in cm

V_* is the shear velocity which is given by $(g.h.S)^{1/2}$.

g is the gravity constant in cm/s^2

h is the depth in cm

S is the energy slope for steady uniform flow.

No design changes in the sampler are required nor should be introduced.

T. Milne Dick
Chief, Hydraulics Division

PERSPECTIVE DE GESTION

On a fait cette étude afin d'examiner la possibilité pour la Division des relevés hydrologiques du Canada d'utiliser des échantillonneurs en forme de panier pour évaluer les paramètres de transport des sédiments dans les cours d'eau, tels que déterminés par la charge de fond.

Les résultats révèlent que le rapport du débit mesuré au débit réel est constant pour une gamme de valeurs d'une variable de contrôle sans dimensions $t_* U_* / L_b$. Lorsque cette variable est supérieure à 30, le rendement est de 30%.

La pratique actuelle, fondée sur un rendement de 30%, est donc confirmée, dans la mesure où on choisit un temps d'échantillonage tel que $t_* U_* / L_b$ soit compris entre 30 et 90.

Dans cette expression:

t_* est le temp d'échantillonnage en secondes

L_b est la longueur de l'échantillonneur en cm

U_* est la vitesse de cisaillement qui est donnée par $(g.h.S)^{1/2}$

où g est l'accélération due à la pesanteur en cm/s^2

h est la profondeur en cm

S est la pente nécessaire pour entretenir un écoulement uniforme.

Aucun changement dans la conception de l'échantillonneur ne doit ou ne devrait être apporté.

T. Milne Dick, chef
Division d'hydraulique

1.0 INTRODUCTION

Basket type bed load samplers are used by the Water Survey of Canada and other agencies to measure the rate of transport of bed material in gravel bed streams. The rate of bed load transport is obtained from samples taken at selected points in a given cross secton. Measuring the weight of the trapped sediment and knowing the duration of sampling, the specific bedload discharge per unit width of bed at each sampling point is determined. Standard procedures are then used to obtain the average bed load discharge for the entire cross section from the sampled points.

The difficulty in the use of samplers arises because they trap less than the amount of material that would pass had the sampler not been there. The basic problem is that the flow passing through the sampler is subject to hydraulic losses and these increase as the sampler fills up. This is further complicated because the presence of the sampler on the stream bed alters the flow patterns and bed load movement in its vicinity. As a result, samplers must be calibrated to determine their trapping efficiency under the different conditions that affect them.

In view of these problems, investigators have searched for alternative methods but so far have had only limited success. Methods, such as the use of tracers (Hubbel and Sayre, 1963; Nelson and Coakley, 1974), acoustic devices (Jonys, 1976) and excavated pits (Murphy and Amin, 1979; Waslenchuck, 1976) have been attempted. These have either failed to work or are too costly and impractical. Methods using dune profile measurements have given good results in flume tests (Engel and Lau, 1980; Engel and Wiebe, 1979) but must still be further investigated.

It appears that, for some time to come, data gathering agencies such as the Water Survey of Canada will be using bed load samplers. In this report, the trapping characteristics of the Water Survey of Canada (WSC) basket type sampler are examined and its sampling efficiency determined. This study was requested by the Water

Survey of Canada and was conducted as part of the research work of the Hydraulics Division of the National Water Research Institute.

2.0 ANALYTICAL CONSIDERATIONS

The amount of material trapped in a sampler depends on the sampling time, flow conditions, bed material properties and the geometric characteristics of the sampler. It is obvious from physical reasoning that, as the sampler fill up, the rate at which it traps material must slow down. In general, a sampler should not be allowed to become more than half full. At the same time, one must also take care not to collect too small a quantity of bed material to ensure that the sample is representative of the true rate of bed load transport. It is therefore useful to have some idea of the rate at which the sampler fills as well as its sampling efficiency.

2.1 Sampler Catch

Considering a two-dimensional, tranquil and uniform flow, the volume of bed material, including the voids, trapped by the sampler may be expressed as

$$V_D = F_1 \left[U_*, h, t_*, D_{50}, \rho_s, \psi, \rho, \mu, \gamma_s, L_a, L_b, L_c \right] \qquad (1)$$

in which V_D = volume of bed material,including the voids, trapped in the sampler, F_1 denotes a function, U_* = shear velocity (the shear velocity $U_* = (g.hS)^{1/2}$ where S is the energy slope for steady state and g is gravity constant), h = depth of flow, t_* = length of sampling time, D_{50} = median grain size, ρ_s = density of the bed material, ψ = grain size distribution factor given as $\psi = D_{84}/D_{16}$, ρ = density of the fluid, μ = viscosity of the fluid, γ_s = specific weight of the bed material, L_a, L_b, L_c = height, length and width of the sampler respectively. Using dimensional analysis one obtains

$$\frac{V_D}{L_a L_b L_c} = F_2 \left[\frac{h}{D_{50}}, \frac{t_* U_*}{L_b}, \frac{\rho_s}{\rho}, \psi, \frac{U_* D_{50} \rho}{\mu}, \frac{\rho U_*^2}{\gamma_s D_{50}}, \frac{D_{50}}{L_a}, \frac{L_b}{L_a}, \frac{L_c}{L_a} \right] \qquad (2)$$

It has been shown by Engel and Lau (1980b) that h/D_{50}, ρ_s/ρ, $U_* D_{50}\rho/\mu$ can be eliminated from Equation 2. In addition L_b/L_a and L_c/L_a for this sampler are constant and may also be eliminated from further consideration. Writing the total sampler volume as $V_t = L_a L_b L_c$, Equation 2 can be written in the reduced form of

$$\frac{V_D}{V_t} = F_3 \left[\frac{t_* U_*}{L_b}, \frac{\rho U_*^2}{\gamma_s D_{50}}, \frac{D_{50}}{L_a}, \psi \right] \qquad (3)$$

Equation 3 shows that the sampler catch should depend on four dimensionless, independent variables.

2.2 Sampling Efficiency

The sampling efficiency of the samplers is defined as the ratio of the measured transport rate to the actual transport rate at the sampling location if the sampler had not been there. This efficiency can be expressed in terms of the same independent variables given in Equation 1, resulting in

$$E = \phi_1 \left[U_*, h, t_*, D_{50}, \rho_s, \psi, \rho, \mu, \gamma_s, L_a, L_b, L_c \right] \qquad (4)$$

in which E = sampling efficiency expressed in percent, ϕ denotes a function and the other variables have been previously defined. Dimensional considerations yield the relationship

$$E = \phi_2 \left[\frac{h}{D_{50}}, \frac{t_* U_*}{L_b}, \frac{\rho_s}{\rho}, \psi, \frac{U_* D_{50}\rho}{\mu}, \frac{\ell U_*^2}{\gamma_s D_{50}}, \frac{D_{50}}{L_a}, \frac{L_b}{L_a}, \frac{L_c}{L_a} \right] \qquad (5)$$

Once again h/D_{50}, ρ_s/ρ, $U_* D_{50}\rho/\mu$, L_b/L_a and L_c/L_a may be omitted from further consideration since their effects will not significantly affect the dependent variable. The sampling efficiency can now be expressed as

$$E = \phi_3 \left[\frac{t_* U_*}{L_b}, \frac{\rho U_*^2}{\gamma_s D_{50}}, \frac{D_{50}}{L_a}, \psi \right] \quad (6)$$

Equations 3 and 6 show that, based on dimensional considerations alone, the sampler catch V_D/V_t and sampling efficiency E should depend on different functions composed of the same independent dimensionless variables. The extent to which this is true must be determined from experimental data.

3.0 EXAMINATION OF EXISTING DATA

Available data which are complete enough to use with Equations 3 and 6 are very limited and the only data set found suitable was that of Gibbs (1973). The data were obtained for three different flow conditions. For each value of t_*, 50 samples were taken with a model basket sampler in a flume at a fixed location at time intervals from 90 seconds - 180 seconds and their average dry weight was determined. The true bed load transport was obtained with a slot sampler located in the flume bed. Sampling with the slot was done at constant intervals of 180 seconds and values of t_* corresponding to those used with the model sampler being tested. The true transport rate was then determined by taking the average dry weight of the 50 samples as before. The averaging of the samples in each case smoothed out the fluctuations in bed load movement due to the presence of dunes. All tests were done on a 1:5 scale model of the basket sampler used by Water Survey of Canada shown in Figure 1. In all cases, the ratio of flume width to sampler width was equal to 10. Also, there was no significant difference in the grain size distributions since ψ was virtually constant at 4.9. In order to determine the sample volume V_D trapped in the basket from the available data,the relationship $V_D = W_D/\rho_s\ (1 - p)$ was used in which W_D = mass of the sample and p = porosity of the granular material. The data from Gibbs (1973) are given in Table 1. The information is used to examine the effect of the four independent dimensionless variables t_*U_*/L_b, $\rho U^2_*/\gamma_s D_{50}$, D_{50}/L_a and ψ on V_D/V_t and E.

V_D/V_t was plotted as a function of t_*U_*/L_b with $\rho U^2_*/\gamma_s D_{50}$ and D_{50}/L_a as parameters in Figure 2. ψ was always constant at 4.9. The plot shows that V_D/V_t increases with t_*U_*/L_b in all cases and that the rate of increase in V_D/V_t decreases as t_*U_*/L_b increases. It is also apparent that this variation for this case of ψ = 4.9 depends on the mobility number $\rho U^2_*/\gamma_s D_{50}$. For the two cases of D_{50}/L_a = 0.084 and 0.086, the corresponding values of $\rho U^2_*/\gamma_s D_{50}$ are 0.123 and 0.074. For

practical purposes, these two values of D_{50}/L_a may be considered to be constant and thus the difference in the two curves of V_D/V_t versus t_*U_*/L_b demonstrate the effect of $\rho U^2_*/\gamma_s D_{50}$ alone. For the greater value of $\rho U^2_*/\gamma_s D_{50}$, there is more material trapped in the sampler for the same value of t_*U_*/L_b as well as a greater rate of decrease in V_D/V_t as t_*U_*/L_b increases. This shows that for a given sampling time t_*, the amount of material deposited in the sampler depends on the rate of bed load transport since this is known to be strongly dependent on the mobility number. The curve for $\rho U^2_*/\gamma_s D_{50} = 0.095$, as one would expect, falls between the curves for which $\rho U^2_*/\gamma_s D_{50} = 0.073$ and 0.123. However, in this case the value of $D_{50}/L_a = 0.106$ is larger than that for the other two curves. Consequently, this curve shows the simultaneous effect of both $\rho U^2_*/\gamma_s D_{50}$ and D_{50}/L_a and does not provide any information about the independent effects of these two variables. Additional tests are required to further define the effect of $\rho U^2_*/\gamma_s D_{50}$ and D_{50}/L_a. Since the data from Gibbs (1973) are all for $\psi = 4.9$, experiments should also be conducted for a different value of ψ.

As a preliminary assessment of the sampling efficiency, E was plotted as a function of t_*U_*/L_b with $\rho U^2_*/\gamma_s D_{50}$ and D_{50}/L_a as parameters in Figure 3 with $\psi = 4.9$ as before. The plot shows that the efficiency decreases as t_*U_*/L_b increases. This is because as t_*U_*/L_b increases, the sample volume V_D/V_t as shown in Figure 2 increases with the result that the hydraulic efficiency of the sampler decreases. When $t_*U_*/L_b < 25$, the rate of decrease in E as t_*U_*/L_b increases is quite significant. When $t_*U_*/L_b \geq 25$, the rate of change in E becomes much smaller as t_*U_*/L_b increases. The fact that the data for the flow conditions tested by Gibbs collapse to form a single curve, indicates that $\rho U^2_*/\gamma_s D_{50}$ is not very important in defining sampling efficiency. The single curve also implies that D_{50}/L_a may not be a significant parameter, however, its value varied only over the narrow

range from 0.084 to 0.106. Therefore, more data are required to determine the separate effect of this variable, as well as to shed more light on the effect of $\rho U^2_*/\gamma_s D_{50}$ and ψ.

4.0 EXPERIMENTAL SET UP AND PROCEDURE

The experiments were conducted in a tilting flume, rectangular in cross section, 2 m wide with glass side walls 0.75 m high and having an overall length of about 22 m. The flume and its auxiliary equipment are described in detail by Engel and Lau (1980a). Two types of granular materials were used for the tests. The first was a river wash sand, fairly uniform in size with a median sieve diameter of 1.1 mm. The second material was a river wash gravel, also fairly uniform in size having a median diameter of 4.8 mm. In both cases, the grains were rounded and their specific gravity was taken to be 2.65 and their average porosity as 0.45.

Two basket samplers were used for the tests with the river wash sand (i.e. D_{50} = 1.1 mm). The dimensions of these samplers are given in Table 2. The samplers were simply identified as A-1 and A-2 in the order from smaller to larger sampler. For both of these samplers, the same standard 0.6 mm stainless steel screen was used. For the tests with the river wash gravel (i.e. D_{50} = 4.8 mm), three samplers were used, designated as B-1, B-2 and B-3 with the order again taken from smallest to largest sampler. All three samplers of the latter set were covered with a 1.4 mm stainless steel screen. The dimensions of these samplers are given in Table 3. As can be seen from Tables 2 and 3, the dimensions of the two samplers A-1, B-1 and A-2, B-2 are the same. This was done to compare baskets of one size when used in bed material of different sizes. In all cases, the samplers were suspended by a rod which was connected to the top of each sampler with a swivel joint. This permitted the samplers to be placed lightly on the bed and to have them align themselves freely with the bed contours.

The experiments were divided into runs and sampling sequences. A run was a test for a specific flow condition and consisted of several sampling sequences for each sampler. A run was set up as described by Engel and Lau (1980a). When equilibrium conditions were reached, several water surface and bed profiles were

taken to obtain the average water surface slope and flow depth from which the shear velocity U_* was computed. Once this was completed sampling began. Each sampling sequence consisted of 25 samples at a predetermined sampling duration t_* with a two minute time interval being maintained between successive samples (Gibbs, 1973). At the end of each run, the samples were weighed under water and the average submerged mass for each sampling sequence obtained. In order to compute the volume of trapped material V_D (including the voids), the submerged mass was then converted to dry mass by the relationship $W_D = 1.606\ W_S$ (W_S = submerged mass, W_D = dry mass). The factor of 1.606 is the value of the ratio $Sg/(Sg-1)$ in which Sg = the specific gravity of the bed material having a value of 2.65. In all, two runs were made with the river wash sand and three runs were made with the gravel. In all cases, the ratio of flow depth to sampler height was kept large enough so as not to affect the results. Independent measurements of the actual average bed load transport occurring in the flume were obtained in the manner described by Engel and Lau (1980a). The data for the tests are given in Table 4 for the river wash sand and Table 5 for the gravel.

5.0 DATA ANALYSIS

The data in Tables 4 and 5 were used to examine the independent effects of $\rho U^2_*/\gamma_s D_{50}/L_a$ and ψ on the sampler catch V_D/V_t and the sampling efficiency E.

5.1 Sampler Catch

The effect of $\rho U^2_*/\gamma_s D_{50}$ was examined with D_{50}/L_a and ψ held constant at 0.096 and 1.2 respectively. Data were plotted as V_D/V_t versus $t_* U_*/L_b$ for values of $\rho U^2_*/\gamma_s D_{50}$ of 0.073 and 0.098, resulting in two curves shown in Figure 4. The plots show that each curve exhibits the same basic characteristics observed with data from Gibbs (1973) in Figure 2. For a given value of $t_* U_*/L_b > 0$, the curve for the larger value of $\rho U^2_*/\gamma_s D_{50}$ shows the greater value of V_D/V_t, indicating again that sampler catch should increase with an increase in mobility number. In other words, the sampler catch increases as the bed load transport rate increases for the same sampling time t_*. The curves also show again that the rate of increase in V_D/V_t decreases as $t_* U_*/L_b$ increases and is indicative of the increase in hydraulic losses in the sampler. Therefore, care should be taken that the sampler does not become too full, with an upper limit of $V_D/V_t = 0.5$ suggested by Gibbs (1973).

The effect of D_{50}/L_a on the sampler catch was examined for values of $\rho U^2_*/\gamma_s D_{50}$ from 0.081 to 0.085 and values of ψ from 1.2 to 1.4. Since both of these variables vary over a very narrow range they are considered to be constant. Data were plotted as V_D/V_t versus $t_* U_*/L_b$ for values of D_{50}/L_a of 0.014, 0.048 and 0.063 in Figure 5, resulting in three curves. The curves show that, for a given value of $t_* U_*/L_b > 0$, the value of V_D/V_t increases as D_{50}/L_a increases and that this increase is approximately proportional to D_{50}/L_a. This means that, for a given mobility number, grain size distribution and sampler size, the volume

occupied by the trapped material is always greater for larger grain sizes than for smaller sizes. Therefore, depending on the transport rate, shorter sampling times t_* may be required for coarser grain sizes in order to satisfy the criterion $V_D/V_t < 0.5$.

The effect of ψ on the sampler catch was examined using data from Gibbs (1977) in Table 1 and the present experiments in Table 5. Values of V_D/V_t were plotted versus t_*U_*/L_b for values of ψ = 4.9 and 1.2, providing two curves in each of Figures 6 and 7. In Figure 6, values of $\rho U^2_*/\gamma_s D_{50}$ varied only slightly from 0.095 to 0.098 and are considered to be constant. In contrast to this, D_{50}/L_a varied from 0.096 to 0.106 which should not be considered as constant. The plot in Figure 6 shows that, for a given value of $t_*U_*/L_b > 0$, there is a considerable difference in V_D/V_t between the two curves with the curve for the larger ψ and D_{50}/L_a giving the larger value of V_D/V_t. As observed in Figure 5, values of V_D/V_t should increase approximately proportionately with increasing D_{50}/L_a. However, noting the effect of D_{50}/L_a on V_D/V_t in Figure 5, the difference in the two curves in Figure 6 cannot be accounted for by D_{50}/L_a alone. The additional difference between the two curves must therefore be due to the effect of the four-fold increase in ψ from 1.2 to 4.9.

In Figure 7, $\rho U^2_*/\gamma_s D_{50}$ again varied only slightly going from 0.073 to 0.074 and hence can be considered to be constant. In this case, values of D_{50}/L_a were 0.086 and 0.096 which is too wide a range to be considered constant. The plot of V_D/V_t versus t_*U_*/L_b shows only a small difference between the two curves. In contrast to previous observations, this time the curve with the lower value of D_{50}/L_a gives the higher value of V_D/V_t for the same value of t_*U_*/L_b, whereas it should have given a lower value. This shift in the curve for which D_{50}/L_a = 0.086 must be due to the fact that it represents a value of ψ which is four times larger than that of the curve for which D_{50}/L_a = 0.096. This again shows that the effect of increasing ψ is to increase the sampler catch for a given mobility number.

In summary, considering the analysis of the data, the dimensionless sampler catch V_D/V_t must be considered to be dependent on t_*U_*/L_b, $\rho U^2_*/\gamma_s D_{50}$, D_{50}/L_a and ψ as indicated by Equation 3. Knowledge of their relative effects on the sampler catch is sufficient for practical purposes and no further tests are required.

5.2 Sampling Efficiency

It was shown in Figure 3 that, over the narrow range of D_{50}/L_a = 0.084 to 0.086, there was no effect of $\rho U^2_*/\gamma_s D_{50}$ over its range from 0.074 to 0.123 on the plot of E versus t_*U_*/L_b. This was the case for constant value of ψ =4.9. In Figure 8, E is plotted versus t_*U_*/L_b for D_{50}/L_a = 0.096 which is between the values of D_{50}/L_a = 0.084 and 0.106 shown in Figure 3. In this case, the values of $\rho U^2_*/\gamma_s D_{50}$ are 0.073 and 0.098 for ψ = 1.2. Once again, the results show that there is no effect of $\rho U^2_*/\gamma_s D_{50}$, even though in this case ψ is four times smaller. This further substantiates the findings by Engel and Lau (1980b) that the sampling efficiency is not dependent on the transport rate as reported by Gibbs (1973). Instead the increase in efficiency at higher transport rate reflects the decrease in sampling time t_* rather than the increase in transport rate. At higher transport rates, the sampling time t_* for a given sampler must be shorter to avoid "overfilling".

The effect of D_{50}/L_a on sampling efficiency was examined for values of ψ = 1.2 and 1.4 which again may be considered to be constant. The range in $\rho U^2_*/\gamma_s D_{50}$ was from 0.081 to 0.104, however, since the sampling efficiency is not affected by the mobility number, this range of values is of no consequence. Data were plotted as E versus t_*U_*/L_b for values of D_{50}/L_a = 0.014, 0.022, 0.048 and 0.063 in Figure 9. The plot shows that data for D_{50}/L_a = 0.048 and 0.063 could be fitted by a single curve, whereas a separate curve was needed to define the data for each of D_{50}/L_a = 0.014 and

0.022, giving a total of three curves. Comparison of the three curves shows that there is an effect of D_{50}/L_a when its value is below some value less than 0.048 resulting in an increase in efficiency as D_{50}/L_a decreases over the range of t_*U_*/L_b tested. This confirms speculations on the effect of D_{50}/L_a on E made by Engel and Lau (1981). It is also in agreement with the fact that for a given V_D/V_t and flow condition, a decrease in D_{50}/L_a will result in an increase of hydraulic efficiency. The difference between the curves is largest at small values of t_*U_*/L_b and decreases as t_*U_*/L_b increases. This effect increases as D_{50}/L_a decreases in the range of $D_{50}/L_a < 0.048$.

The effect of ψ on the sampling efficiency was examined using data from Gibbs (1973) in Table 1 and the present experiments in Table 5. Values of E were plotted versus t_*U_*/L_b in Figure 10 with values of D_{50}/L_a varying from 0.086 to 0.106 for ψ = 4.9 and D_{50}/L_a = 0.096 for ψ = 1.2. Once again the mobility number was omitted from considerations for reasons already established. The data in Figure 10 can be described by a single average curve. In the case where ψ = 4.9, the single curve indicates, as seen in Figure 9, that D_{50}/L_a is not significant in this range of D_{50}/L_a. The fact that the data for ψ = 1.2 and D_{50}/L_a = 0.096 also belong to the same curve therefore indicates that the sampling efficiency is not dependent on the grain size distribution.

The analysis has shown that the sampling efficiency is not dependent on $\rho U^2_*/\gamma_s D_{50}$ and ψ. Therefore the sampling efficiency can be expressed in terms of two dimensionless independent variables by the general relationship

$$E = \phi_4 \left[\frac{t_*U_*}{L_D}, \frac{D_{50}}{L_a} \right] \qquad (7)$$

Equation 7 is plotted in Figure 11 as E versus t_*U_*/L_b with D_{50}/L_a as a parameter using all the data in Tables 1, 4 and 5.

Values of D_{50}/L_a varied from 0.014 to 0.106. The plot shows that separate curves can be fitted to the data for D_{50}/L_a = 0.014 and 0.022 and $D_{50}/L_a \geq 0.048$ showing, as in Figure 9, the trend of decreasing E with increasing t_*U_*/L_b as well as the decrease in E as D_{50}/L_a increases. When D_{50}/L_a has reached a value of 0.048, further increasing D_{50}/L_a does not have any effect on the sampling efficiency.

When sampling on a river bed, it is most likely that $D_{50}/L_a > 0.048$. Therefore, for practical application, the efficiency of the WSC basket sampler is a function only of one independent variable, namely, t_*U_*/L_b, and can be expressed in general as

$$E = \phi_5 \left[\frac{t_*U_*}{L_b} \right] \qquad (8)$$

Equation 8 is plotted separately for $D_{50}/L_a \geq 0.048$ in Figure 12 and is recommended for application with the basket sampler used by the Water Survey of Canada. In the range of $30 \leq t_*U_*/L_b \leq 90$, the efficiency decreases smoothly from about 33% to 25%. Considering experimental error in defining the curve, and the uncertainty in measurement of bed load, it is not unreasonable to assume an average efficiency of 30% when $30 \leq t_*U_*/L_b \leq 90$. This value is considerably less than the value of 45% suggested by Hubbel (1964) for different types of basket samplers and the values of 65%, 40% and 60% suggested by Novak (1957) for the "wire mesh" type, "Nesper" type and "Ehrenberger" type. When t_*U_*/L_b decreases below the value of 30, the rate of increase in efficiency increases as t_*U_*/L_b becomes smaller. It is only for $t_*U_*/L_b \leq 10$ that the values of efficiency recommended by Hubbel (1964) and Novak (1957) are realized.

6.0 CONCLUSIONS

6.1 The volume of bed material trapped in the WSC sampler depends on the four dimensionless independent variables t_*U_*/L_b, $\rho U^2_*/\gamma_s D_{50}$, D_{50}/L_a and ψ.

6.2 The sample volume increases with t_*U_*/L_b but the rate of increase decreases as t_*U_*/L_b increases.

6.3 The sample volume for a given sampling time increases as $\rho U^2_*/\gamma_s D_{50}$ increases.

6.4 For a given flow condition and sampling time, the sampler catch increases as D_{50}/L_a increases.

6.5 For a given flow condition, sampling time and median grain size, the sampler catch is greater for a graded bed material than a uniform bed material (i.e. larger value of ψ).

6.6 In general, the sampling efficiency depends on t_*U_*/L_b and D_{50}/L_a. For the range of values tested, when $D_{50}/L_a > 0.048$, the sampling efficiency depends only on t_*U_*/L_b.

6.7 The sampling efficiency decreases as t_*U_*/L_b increases. For values of $t_*U_*/L_b < 30$, the rate of decrease in the efficiency with increase in t_*U_*/L_b is quite large. For values of $t_*U_*/L_b > 30$, the rate of decrease in efficiency is quite small and fairly uniform as t_*U_*/L_b increases.

6.8 For practical application, when $30 \leq t_*U_*/L_b \leq 90$, an average efficiency of 30% may be used.

REFERENCES

Einstein, H. A., 1937. "Die Eicheng der im Rhein Verwendeten Geschiebefaengers (Calibration of Bed Load Samplers Used on the Rhein)". Schweitzer Bauzeitung 110 (12).

Engel, P. and Wiebe, K, 1979. "A Hydrographic Method for Bed Load Measurement". In: River Basin Management (Proceedings 4th National Hydrological Technical Conference, Canadian Society for Civil Engineers, May 7-8, Vol. 1, pp. 98-112.

Engel, P. and Lau, Y. L., 1980a. "Computation of Bed Load Using Bathymetric Survey Data". Journal of the Hydraulics Division, ASCE, Vol. 106, No. 3, Proceedings 15255, pp. 369-380.

Engel, P. and Lau, Y. L., 1980b. "Calibration of Bed Load Samplers". Journal of the Hydraulics Division, ASCE, Vol. 106, No. 10, Proceedings 15725, pp. 1677-1685.

Engel, P. and Lau, Y. L., 1981. "The Efficiency of Basket Type Bed Load Samplers". Erosion and Sediment Transport Measurement, Proceedings of the Florence Symposium, IAHS Publication No. 133, pp. 27-34.

Gibbs, C. J., 1973. "Model Study of the Basket Type Bed Load Sampler". M. Sc. Thesis, University of Alberta, Edmonton, Alberta, Canada.

Hubbel, D. W. and Sayre, W. W., 1963. "Application of Radioactive Tracers in the Study of Sediment Measurement". Proceedings Federal International Agency Sediment, Conference Miscellaneous Publication No. 970, Agricultural Research Service Paper No. 61, pp. 569-585.

Hubbel, D. W., 1964. "Apparatus and Techniques for Measuring Bed Load". USGS Water Supply, Paper No. 1748, U.S. Government Printing Office, Washington, D.C., U.S.A.

Jonys, C. D.,1976. "Acoustic Measurement of Sediment Transport". Scientific Series No. 66, Inland Waters Directorate, Canada Centre for Inland Waters, Burlington, Ontario, Canada.

Murphy, P. Y. and Ain, I. M., 1979. "Compartmented Sediment Trap". Journal of the Hydraulics Division, ASCE, Vol. 105, No. 5, Proceeding 14577, pp. 489-500.

Nelson, D. E. and Coakley, J. P., 1974. "Techniques for Tracing Sediment Movement". Scientifice Series No. 32, Inland Waters Directorate, Canada Centre for Inland Waters, Burlington, Ontario, Canada.

Novak, P., 1957. "Bed Load Meters - Development of a New Type and Determination of Their Efficiency with the Aid of Scale Models". IAHR, 7th General Meeting, Lisbon, Portugal, Trans., Vol. 1, pp. A9-1 - A9-11.

Waslenchuk, D. G., 1976. "New Diver Operated Bed Load Sampler". Journal of Hydraulics Division, ASCE, Vol 102, No. 6, Proceedings 12179, pp. 747-757.

ACKNOWLEDGEMENT

The writer is grateful to John Dalton who prepared all the experiments and assisted in the measurements.

TABLES

TABLE 1. EXPERIMENTAL RESULTS FROM GIBBS (1973)

D_{50} mm	h cm	S	U_* cm/s	t_* s	W_S gm	$\frac{V_D}{V_t}$	E %	$\frac{t_* U_*}{L_b}$	$\frac{\rho U_*^2}{\gamma_s D_{50}}$	$\frac{D_{50}}{L_a}$	ψ
5.3	18.0	0.0046	9.0	30	214.02	0.164	36.9	17.7	0.095	0.106	4.9
5.3	18.0	0.0046	9.0	45	317.71	0.244	36.4	26.6	0.095	0.106	4.9
5.3	18.0	0.0046	9.0	60	386.08	0.296	33.2	35.5	0.095	0.106	4.9
4.3	18.0	0.0029	7.2	60	108.28	0.083	30.1	28.4	0.074	0.086	4.9
4.3	18.0	0.0029	7.2	120	217.01	0.166	30.1	56.8	0.074	0.086	4.9
4.3	18.0	0.0029	7.2	180	263.41	0.202	24.0	85.3	0.074	0.086	4.9
4.2	17.0	0.0050	9.1	10	157.99	0.121	49.1	6.0	0.123	0.084	4.9
4.2	17.0	0.0050	9.1	20	266.14	0.204	41.4	12.0	0.123	0.084	4.9
4.2	17.0	0.0050	9.1	30	357.21	0.274	37.1	18.0	0.123	0.084	4.9
5.3	18.0	0.0046	9.0	30	215.20	0.165	37.1	17.7	0.095	0.106	4.9
5.3	18.0	0.0046	9.0	45	323.88	0.248	36.7	26.6	0.095	0.106	4.9
5.3	18.0	0.0046	9.0	60	451.64	0.346	39.0	35.5	0.095	0.106	4.9
4.3	18.0	0.0029	7.2	60	103.78	0.080	28.6	28.4	0.074	0.086	4.9
4.3	18.0	0.0029	7.2	120	215.20	0.165	29.6	56.8	0.074	0.086	4.9
4.3	18.0	0.0029	7.2	180	305.09	0.234	28.1	85.3	0.074	0.086	4.9
4.2	17.0	0.0050	9.1	10	169.07	0.130	52.7	6.0	0.123	0.084	4.9
4.2	17.0	0.0050	9.1	20	282.30	0.216	43.9	12.0	0.123	0.084	4.9
4.2	17.0	0.0050	9.1	30	398.25	0.305	41.3	18.0	0.123	0.084	4.9

$\psi = D_{84}/D_{16}$

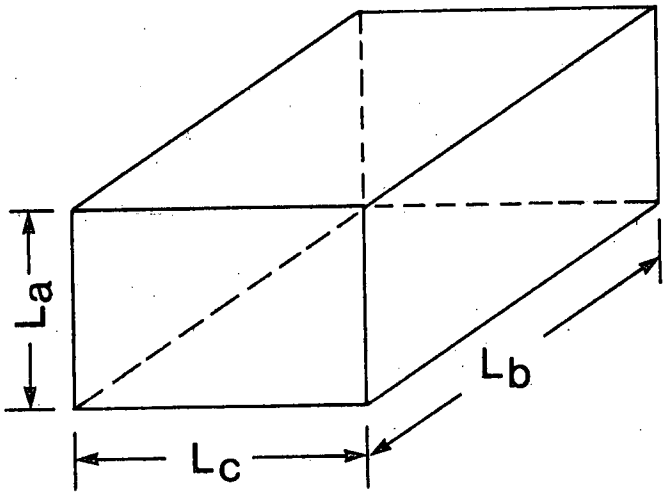

BASKET	L_a(cm)	L_c(cm)	L_b(cm)
A-1	5.0	11.7	15.3
A-2	7.6	17.6	23.6

TABLE 2. BASKET SAMPLERS USED IN TESTS

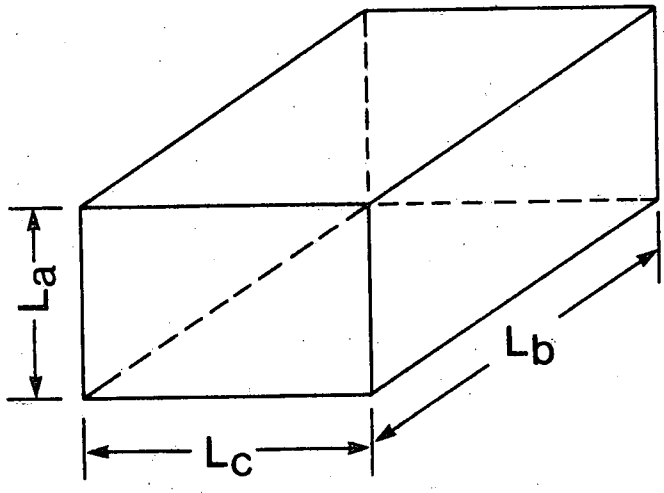

BASKET	L_a (cm)	L_c (cm)	L_b (cm)
B-1	5.0	11.7	15.3
B-2	7.6	17.6	23.6
B-3	9.9	23.0	30.8

TABLE 3. BASKET SAMPLES USED IN TESTS

TABLE 4. EXPERIMENTAL RESULTS FROM TEST SERIES A

D_{50} mm	h cm	S	U_* cm/s	t_* s	W_S gm	$\frac{V_D}{V_t}$	E %	$\frac{t_* U_*}{L_b}$	$\frac{\rho U_*^2}{\gamma_s D_{50}}$	$\frac{D_{50}}{L_a}$	ψ
1.1	14.3	0.00132	4.3	240	83.51	0.064	30.5	67.5	0.104	0.022	1.4
1.1	14.3	0.00132	4.3	180	73.56	0.056	35.8	50.6	0.104	0.022	1.4
1.1	14.3	0.00132	4.3	120	53.96	0.041	39.4	33.7	0.104	0.022	1.4
1.1	14.3	0.00132	4.3	60	37.10	0.028	54.1	16.9	0.104	0.022	1.4
1.1	14.3	0.00132	4.3	180	64.88	0.050	31.6	50.6	0.104	0.022	1.4
1.1	14.3	0.00132	4.3	120	59.26	0.045	43.3	33.7	0.104	0.022	1.4
1.1	14.3	0.00132	4.3	60	32.28	0.025	47.2	16.9	0.104	0.022	1.4
1.1	14.3	0.00132	4.3	30	28.11	0.022	82.1	8.4	0.104	0.022	1.4
1.1	17.1	0.00089	3.9	300	169.43	0.037	38.2	49.6	0.085	0.014	1.4
1.1	17.1	0.00089	3.9	180	122.54	0.027	45.9	29.8	0.085	0.014	1.4
1.1	17.1	0.00089	3.9	120	106.96	0.023	59.6	19.8	0.085	0.014	1.4
1.1	17.1	0.00089	3.9	60	60.39	0.013	67.8	9.9	0.085	0.014	1.4

$\psi = D_{84}/D_{16}$

TABLE 5. EXPERIMENTAL RESULTS FROM TEST SERIES B

D_{50} mm	h cm	S	U_* cm/s	t_* s	W_S gm	$\frac{V_D}{V_t}$	F %	$\frac{t_* U_*}{L_b}$	$\frac{\rho U_*^2}{\gamma_s D_{50}}$	$\frac{D_{50}}{L_a}$	ψ
4.8	17.0	0.00458	8.74	90	352.03	0.270	33.4	51.4	0.098	0.096	1.2
4.8	17.0	0.00458	8.74	60	230.30	0.177	32.8	34.2	0.098	0.096	1.2
4.8	17.0	0.00458	8.74	30	111.59	0.086	31.9	17.1	0.098	0.096	1.2
4.8	17.0	0.00458	8.74	45	153.28	0.118	29.1	25.7	0.098	0.096	1.2
4.8	17.0	0.00322	7.54	180	252.62	0.194	27.4	88.7	0.073	0.096	1.2
4.8	18.0	0.00322	7.54	120	191.28	0.147	31.1	59.1	0.073	0.096	1.2
4.8	18.0	0.00322	7.54	90	159.57	0.122	34.6	44.4	0.073	0.096	1.2
4.8	18.0	0.00217	7.99	240	538.01	0.117	21.6	82.0	0.082	0.063	1.2
4.8	30.0	0.00217	7.99	120	4511.45	0.098	36.3	41.0	0.082	0.063	1.2
4.8	30.0	0.00217	7.99	45	152.91	0.033	32.9	15.4	0.082	0.063	1.2
4.8	30.0	0.00217	7.99	90	260.49	0.057	27.9	30.7	0.082	0.063	1.2
4.8	30.0	0.00217	7.99	180	753.38	0.073	29.8	46.1	0.082	0.048	1.2
4.8	30.0	0.00217	7.99	60	299.68	0.029	35.6	15.4	0.082	0.048	1.2
4.8	30.0	0.00217	7.99	120	452.89	0.044	26.9	30.7	0.082	0.048	1.2

$\psi = D_{54}/D_{16}$

FIGURES

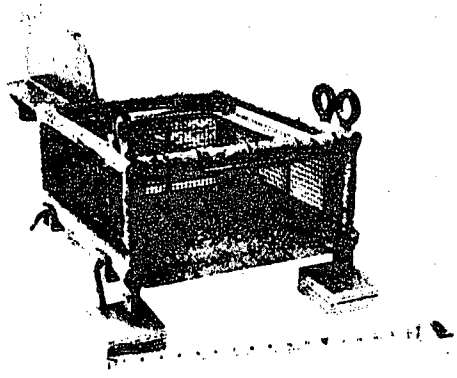

FIGURE 1. W.S.C. BASKET SAMPLER

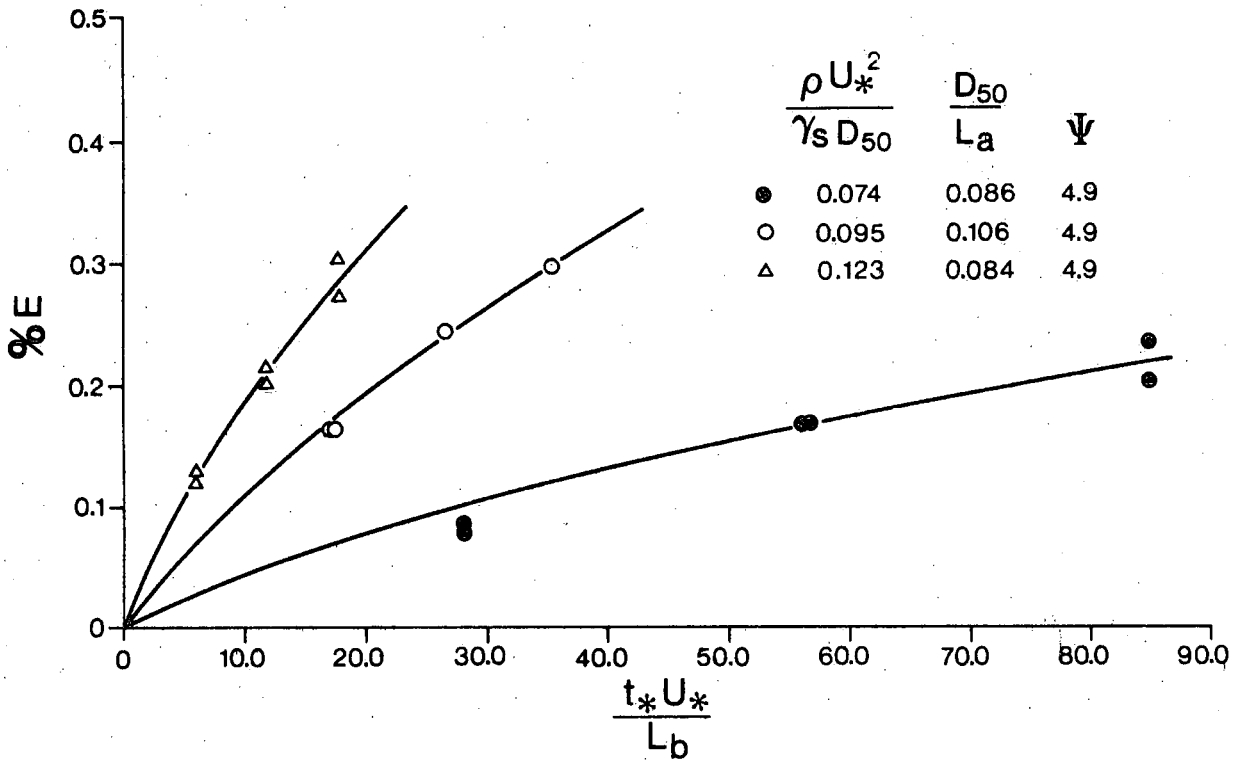

FIGURE 2. VARIATION OF SAMPLER CATCH (from Gibbs, 1973)

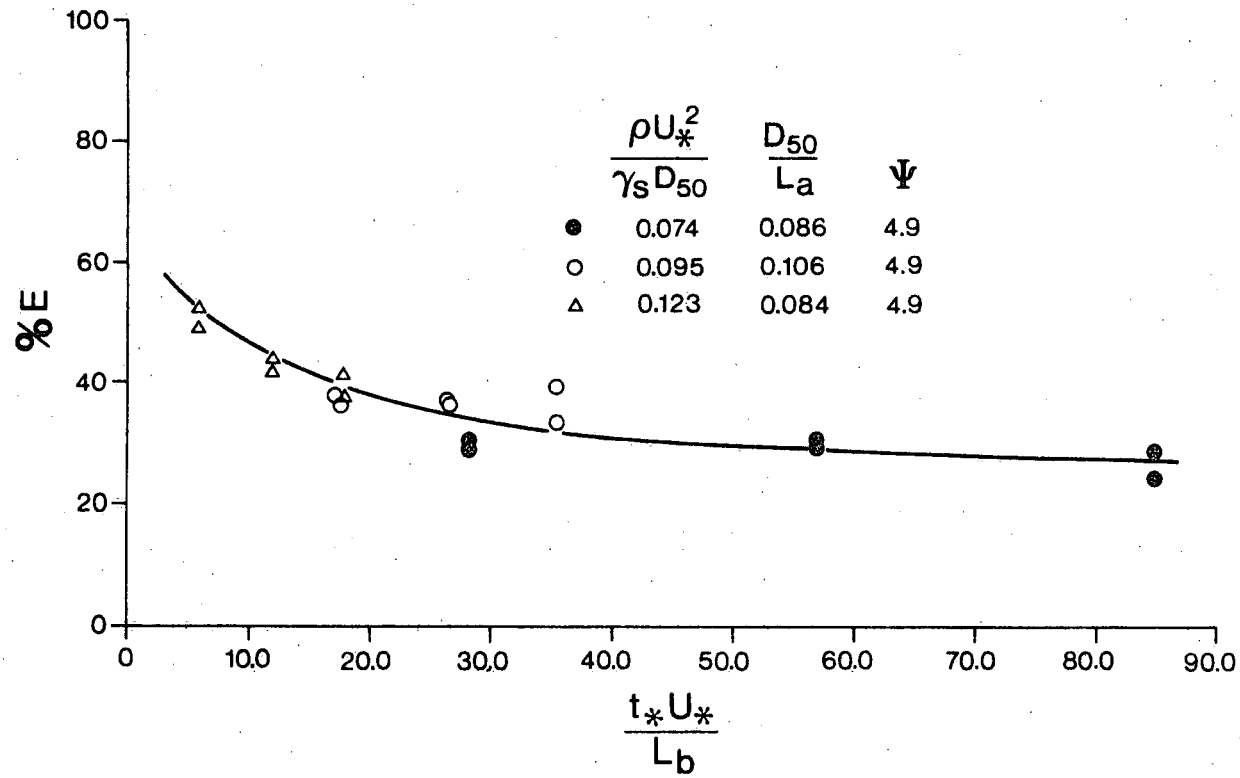

FIGURE 3. VARIATION OF SAMPLING EFFICIENCY (from Gibbs, 1973)

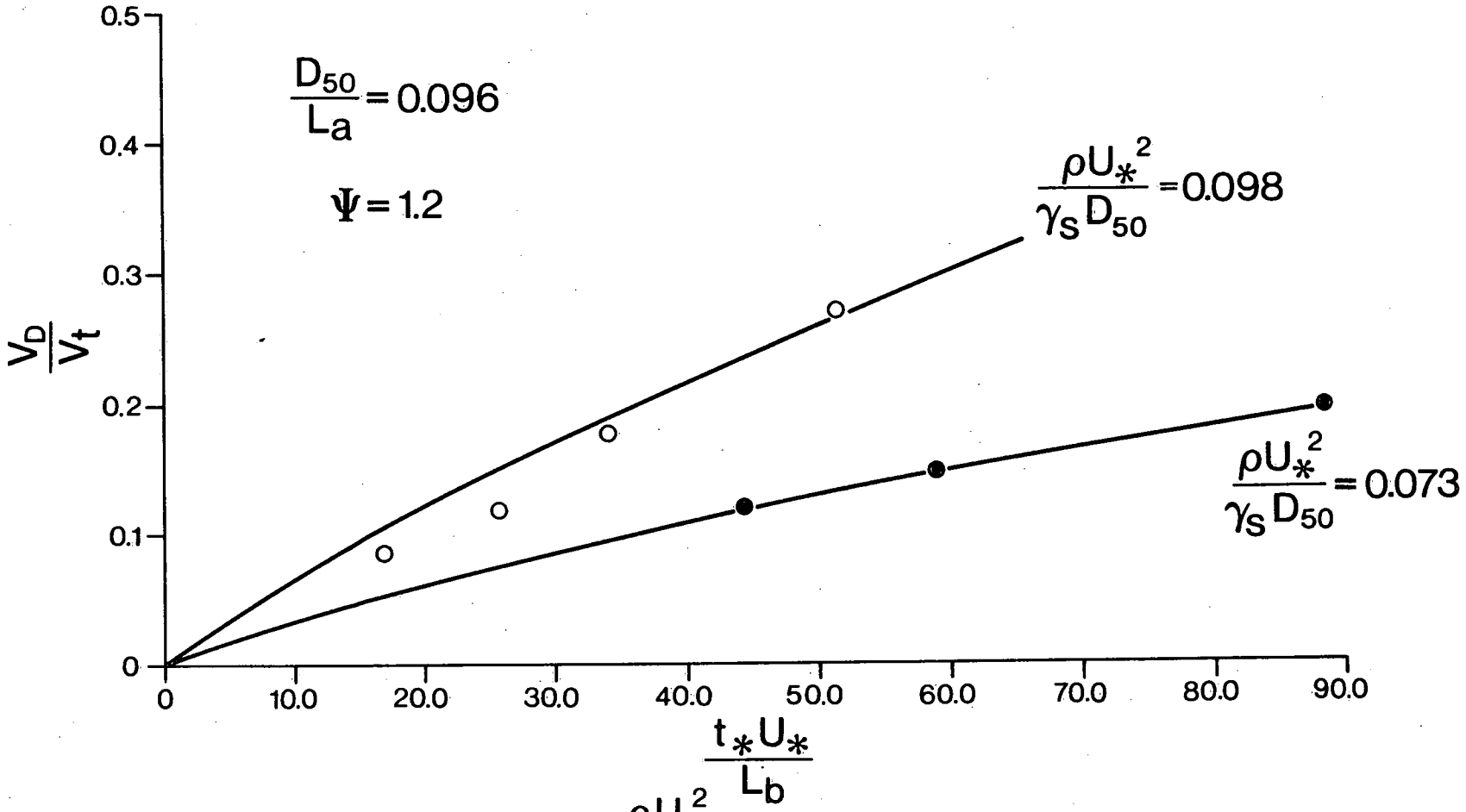

FIGURE 4. EFFECT OF $\frac{\rho U_*^2}{\gamma_s D_{50}}$ ON SAMPLER CATCH

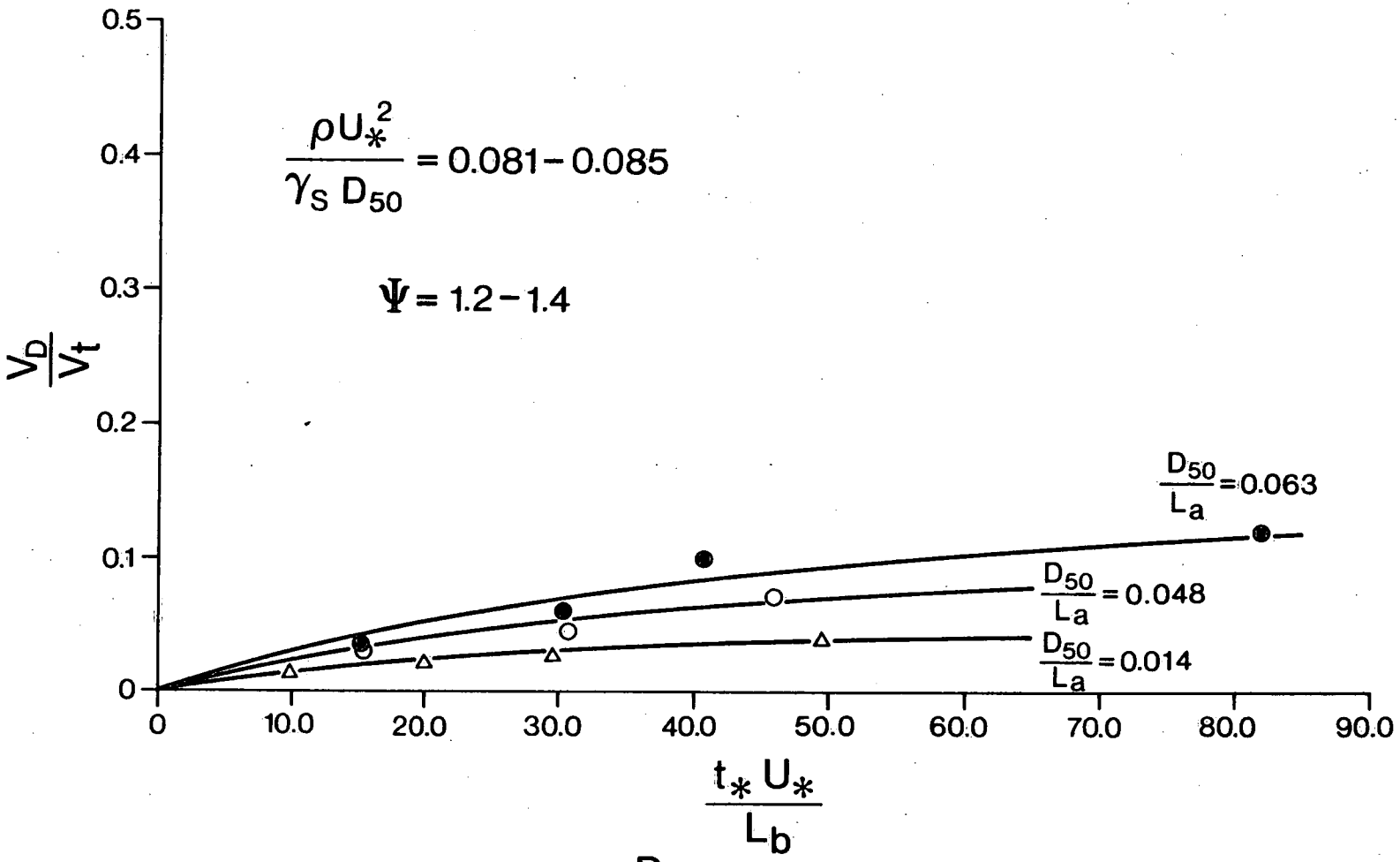

FIGURE 5. EFFECT OF $\frac{D_{50}}{L_a}$ ON SAMPLER CATCH

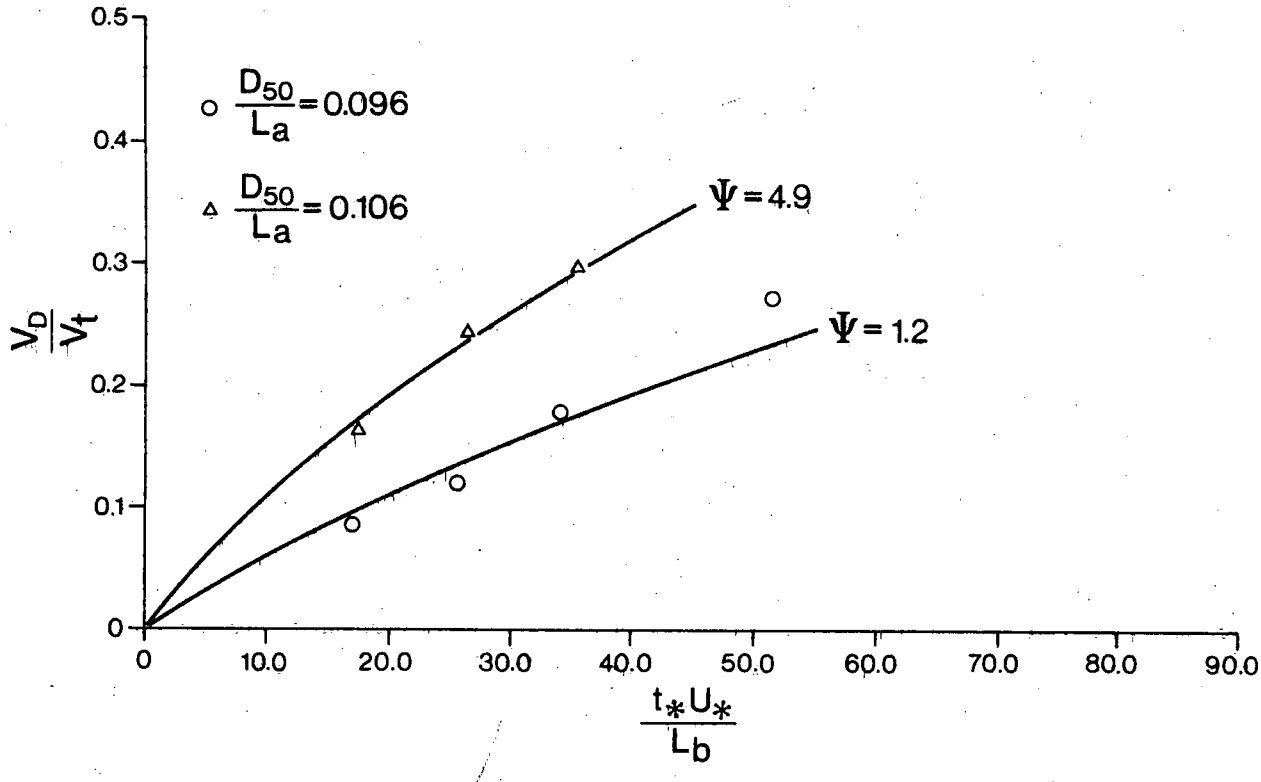

FIGURE 6. EFFECT OF Ψ ON SAMPLER CATCH

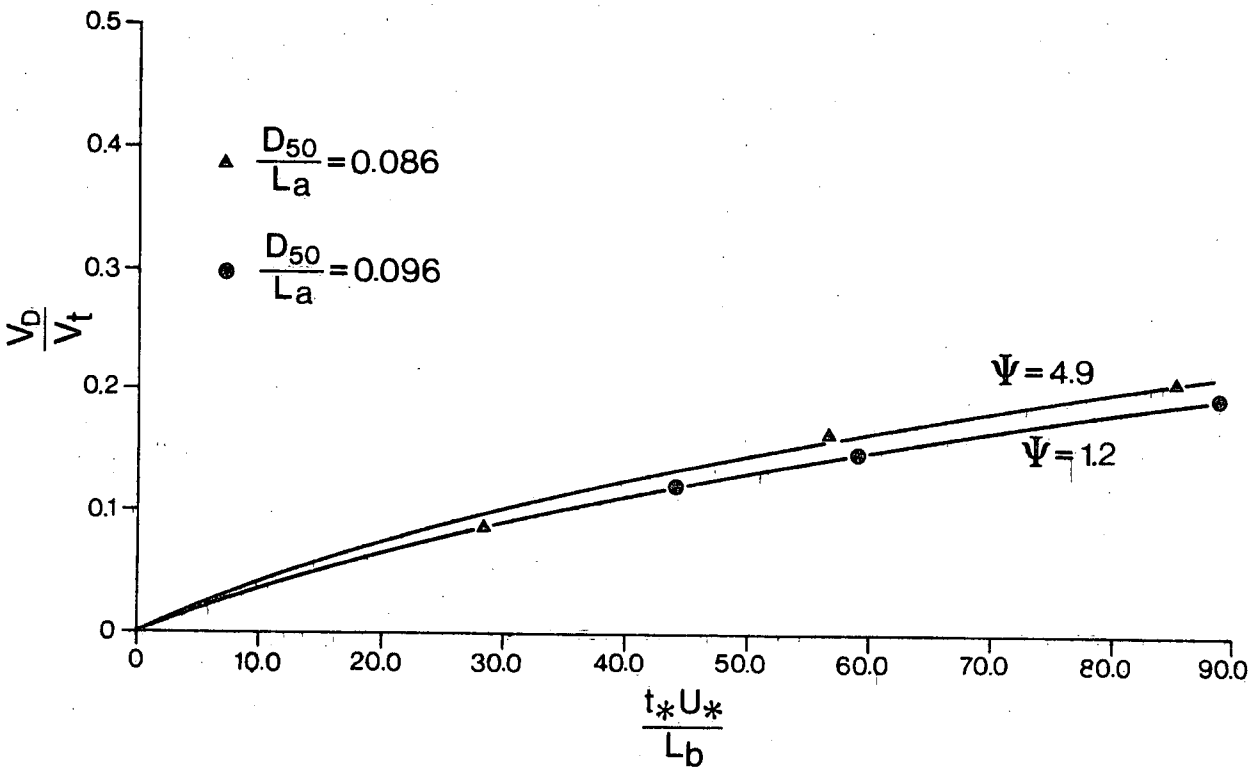

FIGURE 7. EFFECT OF Ψ ON SAMPLER CATCH

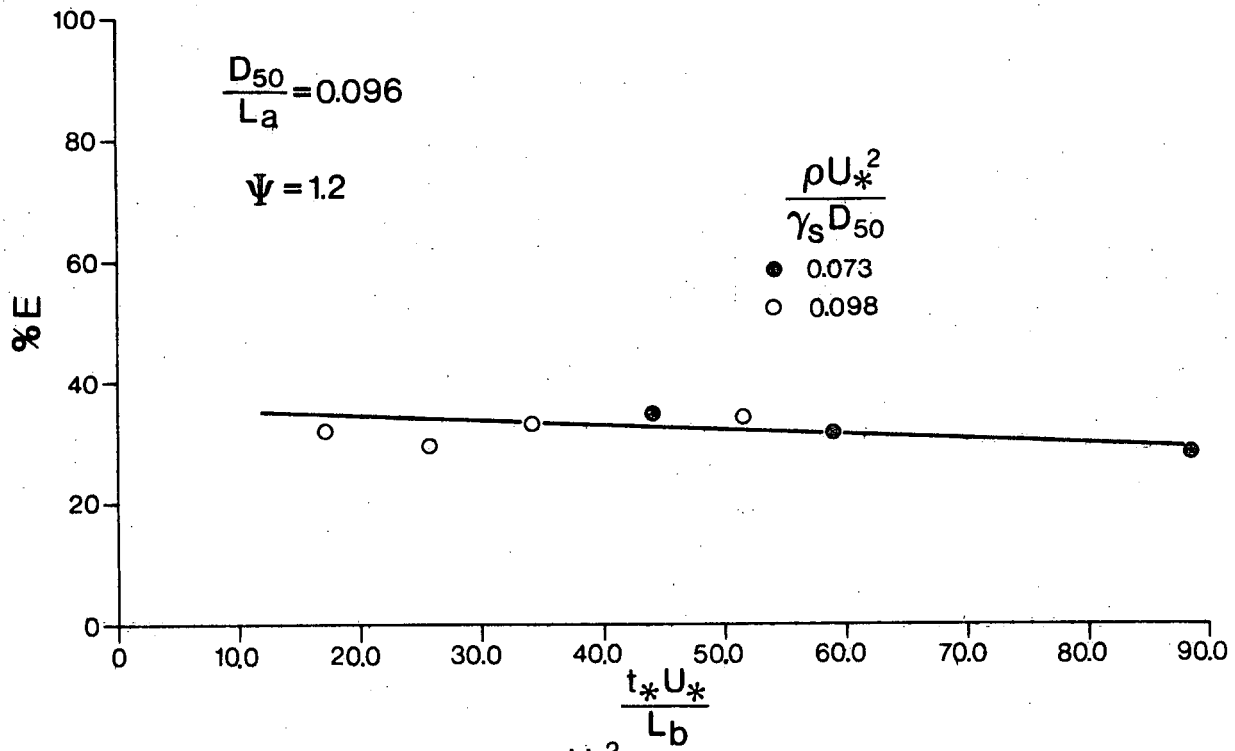

FIGURE 8. EFFECT OF $\frac{\rho U_*^2}{\gamma_s D_{50}}$ ON SAMPLING EFFICIENCY

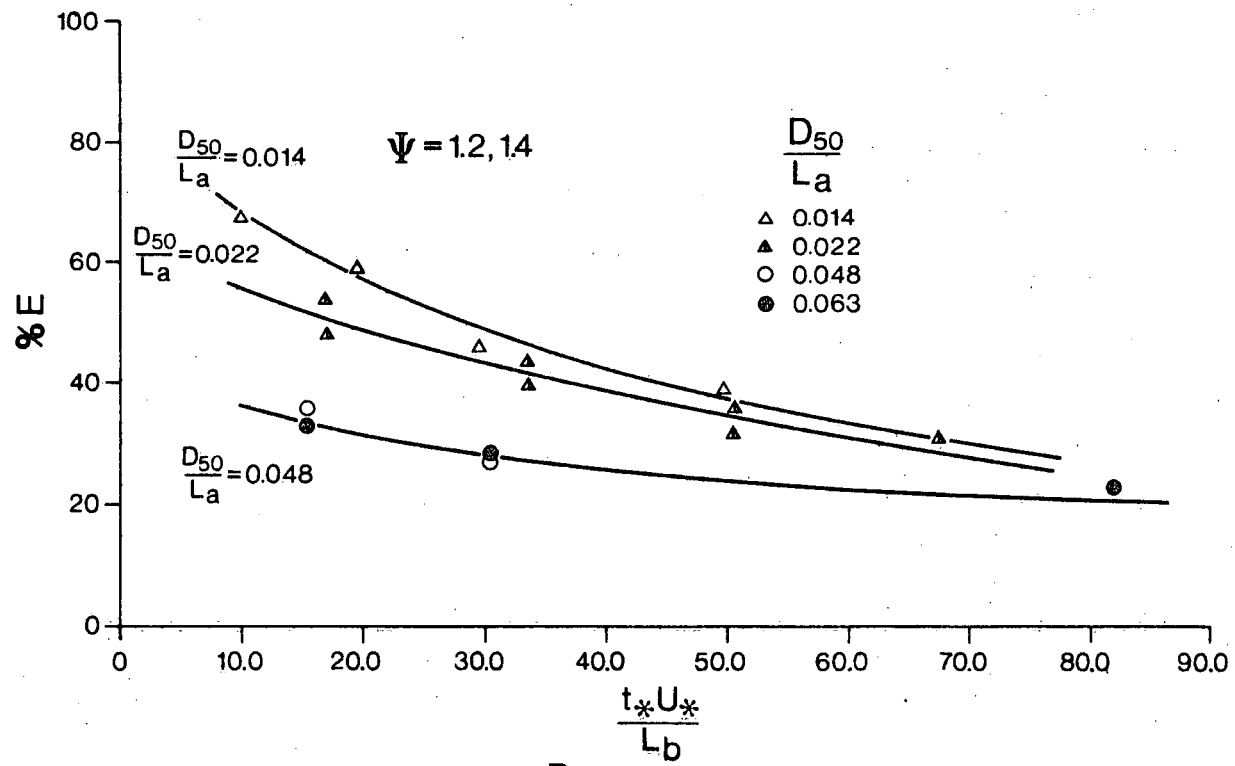

FIGURE 9. EFFECT OF $\frac{D_{50}}{L_a}$ ON SAMPLING EFFICIENCY

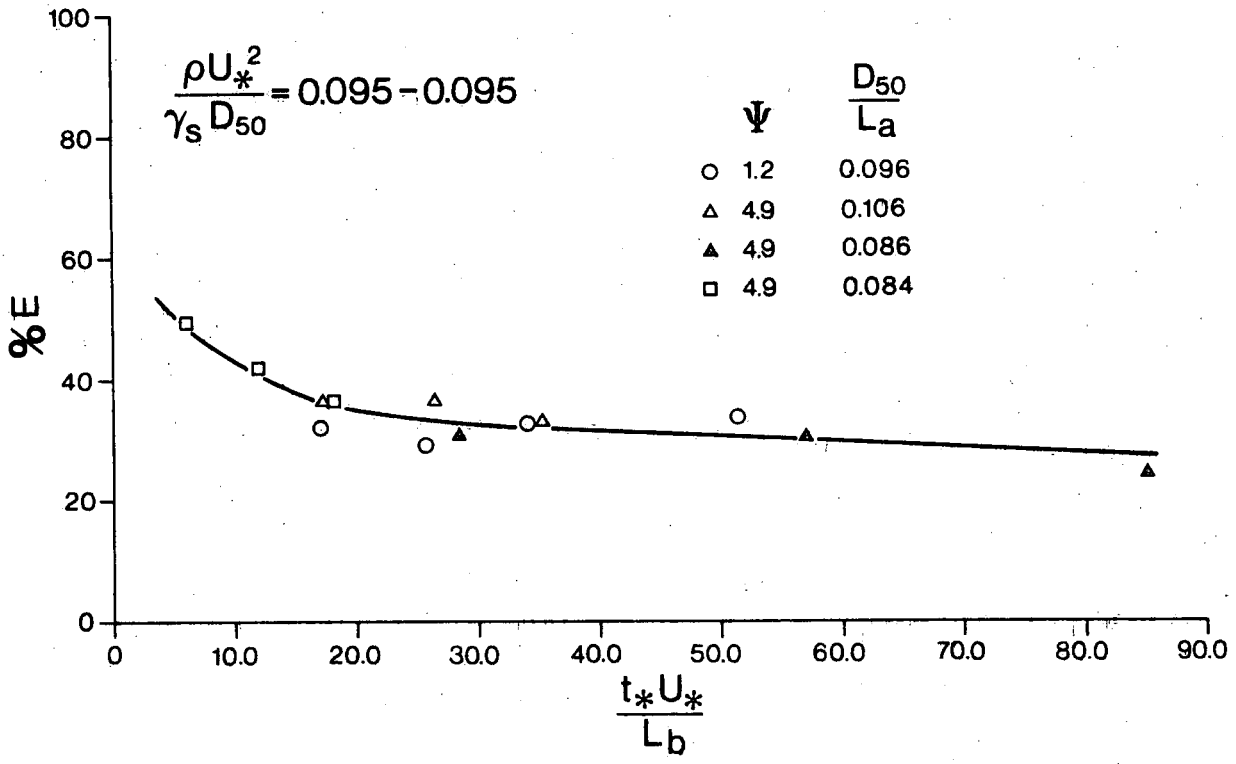

FIGURE 10. EFFECT OF Ψ ON SAMPLING EFFICIENCY

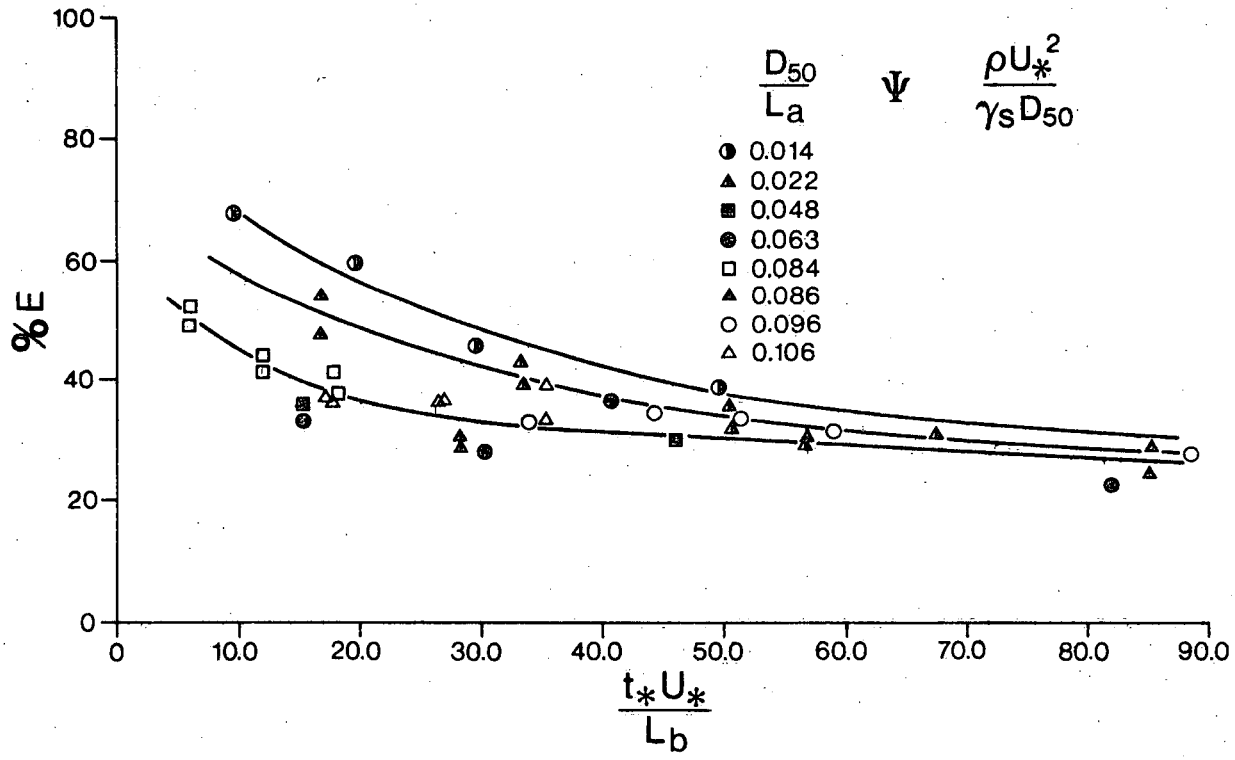

FIGURE 11. VARIATION OF SAMPLING EFFICIENCY

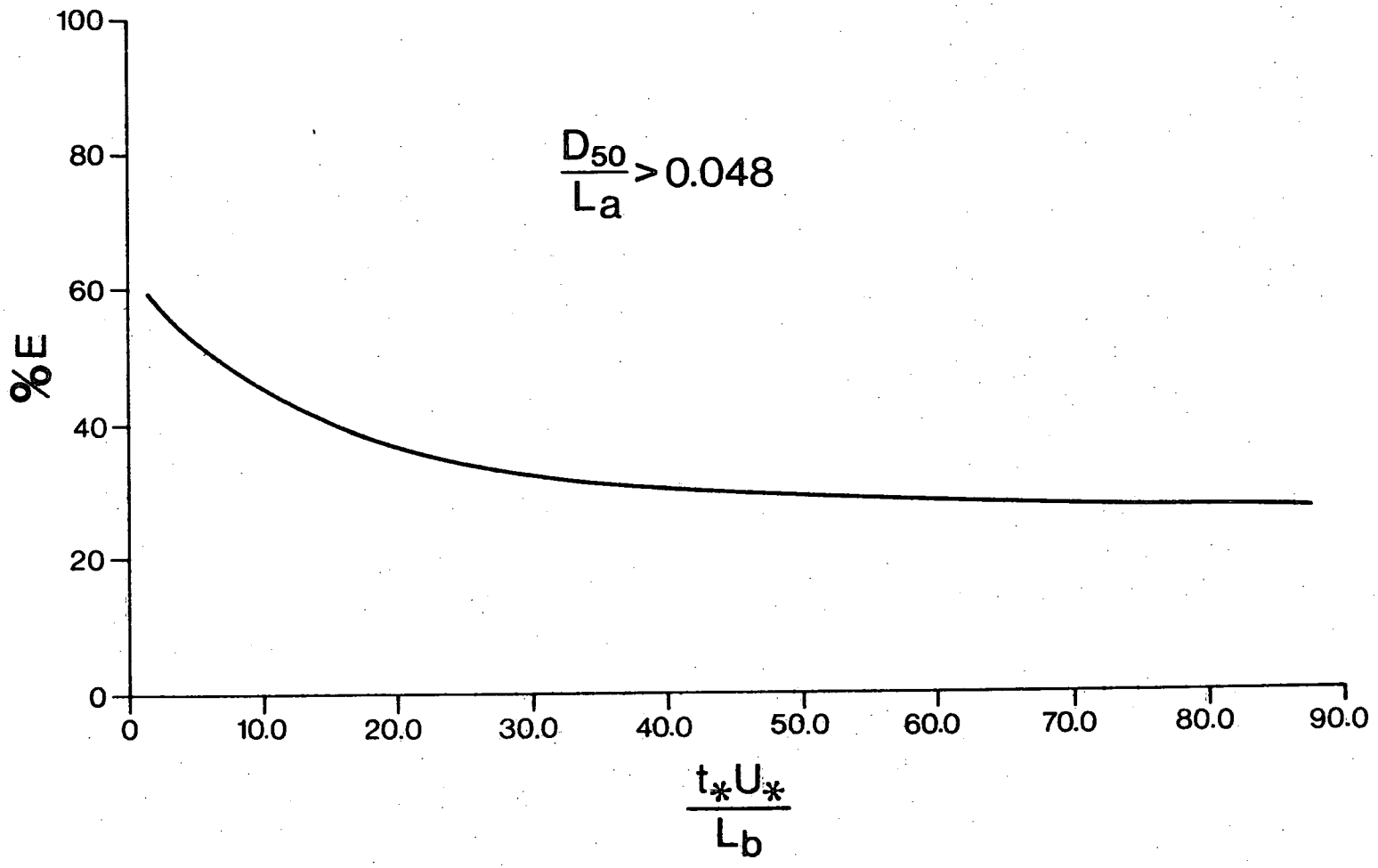

FIGURE 12. CALIBRATION CURVE FOR WSC BASKET SAMPLER